JTTEE5 11:551-558

Examination of the Wear Properties of HVOF Sprayed Nanostructured and Conventional WC-Co Cermets With Different Binder Phase Contents

A.H. Dent, S. DePalo, and S. Sampath

(Submitted 13 December 2000; in revised form 26 March 2001)

There has been an increase in interest of late regarding the properties of thermally sprayed WC-Co cermets with nanograin carbide particles. These powders have shown interesting properties in sintered components, giving high values of hardness (2200-2300 VHN) and improved wear properties. The method used for the processing for these materials—solution formation, spray drying and chemical conversion, rather than introduction of WC as solid particles to a molten binder—allows the formation of sub-100 nm WC particles as a hard second phase.

The work presented here examined the effect of composition on the microstructure and wear properties of some nanostructured WC-Co materials. WC-Co cermets with 8, 10, 12, and 15% Co binder phase were deposited using a Sulzer Metco hybrid DJ HVOF thermal spray system. Optimization of deposition conditions was necessary because of the unique morphology of the powders (thick-shelled hollow spheres) to produce dense consolidated deposits.

There is a higher degree of decarburization of the WC phase in the nanostructured materials compared with the conventional WC-Co. This dissolution of the hard phase is also noted to increase on decreasing binder phase content.

The nanostructured WC-Co coatings have a lower wear resistance compared with the conventional WC-Co for abrasive wear and small particle erosion. The abrasive wear resistance of these nanostructured materials was found to increase on decreasing cobalt binder content. This trend in abrasive wear resistance is consistent with studies on conventional sized cermets and is believed to be more dependent upon proportion of binder phase content than degree of decarburization for the materials studied. The small particle erosion resistance of the nanostructured coatings was found to increase on increasing cobalt content.

Keywords erosive wear, HVOF, nanostructured materials abrasive wear, WC-Co

1. Introduction

WC-Co powders with nanostructured WC grains (20-200 nm) have elicited great interest in recent years because of the novel approach to production of these ultra fine-grained cermets.[1,2] The wear properties of these sintered parts have shown greater resistance to abrasion and sliding wear compared with components with WC crystals of conventional size (1-20 μm).[3,4]

WC-Co cermet powders with WC sizes 1-10 μm are commonly deposited by thermal spray processing as thick protective films of the order of 100-500 μm. Traditionally, this has been accomplished by air plasma spraying (APS), but more recently by the high velocity oxygen fuel (HVOF) process. The HVOF process possesses advantages over APS such as high particle velocities and lower peak particle temperatures, producing a more densely consolidated deposit with reduced formation of detrimental reaction products and correspondingly improved wear properties.[5]

HVOF deposited nanostructured cermets have been studied by a number of researchers.[6,7] However, these coatings have shown larger wear loss in wear studies compared with WC-Co coatings with conventional sized WC grains when deposited under similar conditions.[8] This has been explained in terms of the increased surface area of WC allowing greater degradation and dissolution of this phase, and hence increased proportion of detrimental reaction products. It has been suggested that optimization of spray parameters such that deposition of these materials is achieved at lower temperatures may reduce the degree of degradation of the WC, leading to improved properties. There has been no specific answer however, to whether deposition parameter optimization is able to reduce the dissolution of the WC while still retaining a densely consolidated deposit. The effect of variations in the Co content on the properties of these materials is unclear, and it is not known whether Co contents optimized for conventional cermets should apply also to the nanostructured materials.

This article presents work on four nanostructured WC-Co cermets with different binder phase contents: 8, 10, 12 and 15 wt.% Co. HVOF deposited coatings of these materials were ex-

A.H. Dent, S. DePalo, and **S. Sampath,** Center for Thermal Spray Research, State University of New York at Stony Brook, Stony Brook, NY 11794-2275. Contact e-mail: adent@materialsconnexion.com.

Table 1 Materials Used in This Study

Material Supplier	Designation	Wt.% Cobalt	As-Received Size Distribution (a)
Nanodyne	N-8	8	−103 + 18
Nanodyne	N-10	10	−104 + 16
Nanodyne	N-12	12	−74 + 19
Nanodyne	N-15	15	−110 + 11
Sulzer Metco	C-12	12	−45 + 5

(a) All Nanodyne-supplied materials were screened to 270 mesh prior to deposition.

amined for the effect of binder phase content and also variations in deposition parameter on microstructural development and wear properties. The wear performance of these materials was also compared with deposits produced from a conventional WC-sized commercially available cermet.

2. Experimental Procedure

2.1 Materials

The composition and particle size of the four nanostructured (N-8, N-10, N-12, and N-15) and one conventional (C-12) WC-Co cermet powders used in this study are presented in Table 1. The nanostructured materials were produced by a spray dry and conversion process and were received from Nanodyne Inc. (New Brunswick, NJ). A small variation in the particle size distributions for the powders was noted: the size distributions were found to be larger than generally used as HVOF cuts for these types of cermets. However, all of the Nanodyne-supplied powders were screened using a 270-mesh screen prior to use. The conventional cermet powder was produced by spray drying and sintering.

2.2 HVOF Deposition

Deposition of the four materials was carried out under equivalent conditions using a Sulzer Metco (Westbury, NY) Diamond Jet Hybrid DJ2700 HVOF torch. Propylene was used as a fuel gas utilizing a DJ2700 aircap. The deposition parameters are presented in Table 2. These conditions are those recommended by Sulzer Metco for a conventional sized WC-12Co cermet.[9]

Deposition was onto flat carbon steel substrates rotated on a carousel at a traverse speed of the torch across the substrate of approximately 1 m/s. The standoff distance for the spraying was 230 mm. Four high-pressure air jets were used to produce additional cooling of the substrates. Coatings of 250 μm thick were produced for microscopic examination. In addition, coatings of approximately 750 μm thick were deposited for wear analysis.

2.3 Parameter Optimization

A separate study for parameter optimization was also carried out on the N-15 nanostructured material to attempt to improve the abrasive and erosive wear properties of this class of material. Diagnostic measurements of the velocity and temperature of the particles in flight was used to obtain parameters that achieved velocities equivalent to the standard conditions presented in Table 2, but with lower average particle temperatures. This approach was taken in an attempt to reduce the degree of decarburization of the WC hard phase while achieving similar coating densities. A Tecnar DPV 2000 in-flight particle diagnostic system was used for the parametric study. Measurements of average particle temperature and velocities were taken at 125 mm (~5 in.) and 230 mm (~9 in.) from the torch nozzle exit. Data were averaged over 1500-2000 particles. Table 3 presents the three conditions reached following this study. The geometric setup for this deposition was equivalent to that described above for the Co content study.

Table 2 Standard Deposition Parameters

	Pressure		Flow Rate		
Spray Parameter	KPa	psi	L/min	scfh	FMR
Fuel gas (propylene)	690	100	83	176	40
Oxygen	1034	150	275	578	40
Air	690	100	404	857	48
Nitrogen	690	100	13	28	…
Powder feed rate	…	…	45-50 g/min	…	…

Table 3 Parameter Optimization Conditions for the N-15 Material

Gas Parameter	Fuel-Rich N-15FR	Standard N-15	Oxygen-Rich N-15OR
Oxygen (O_2)			
Pressure, KPa/psi	1034/150	1034/150	1034/150
Flow, L/min	240	275	275
Flow, scfh	505	578	578
Flow, FMR	35	40	40
Propylene (C_3H_6)			
Pressure, KPa/psi	690/100	690/100	690/100
Flow, L/min	85	85	75
Flow, scfh	176	176	154
Flow, FMR	40	40	35
Air			
Pressure, KPa/psi	758/110	690/100	758/110
Flow, L/min	490	405	490
Flow, scfh	1040	857	1040
Flow, FMR	58–60	48	58–60
Percent O_2 stoichiometry (a)	0.64	0.73	0.83

(a) Percent stoichiometry is calculated as fuel-to-oxygen ratio. No account is taken of the supplementary air injected into the flame.

2.4 Microstructural Characterization

To study the material at its different levels of heterogeneity, various microstructural characterization methods were applied. For general phase composition, x-ray diffraction (XRD) was taken of the powders and the top surface of the coatings. Cu Kα radiation was used at 40 kW and 20 mA over a scanning range of 20-60° 2θ.

Light microscopy (LM) and scanning electron microscopy (SEM) in the back-scattered electron mode (BSE) of the surfaces of the powders and the cross sections of the coatings allowed detailed examination of morphology prior to and after deposition of the cermets.

2.5 Wear Analysis

Abrasive wear of the coatings was carried out using an apparatus set up to administer two-body abrasion. Sets of three 20

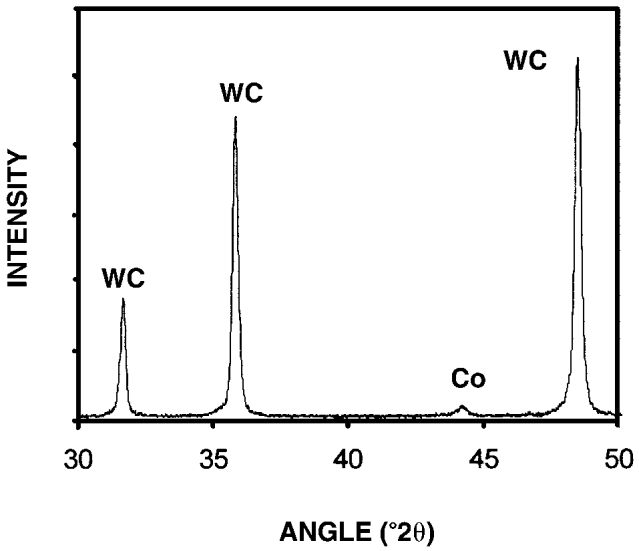

Fig. 1 XRD analysis from the as-received N-12 powder

mm × 20 mm samples were abraded against 120 grit SiC paper in a counter-rotational motion on an auto-polisher. The rotational speed of the abrasive wheel was 300 rpm and the counter speed of the specimen holder was 70 rpm. A total pressure of 240 kPa was applied for the three specimens. Water was introduced onto the sheets at a rate of 760 mL/min. The abrasive sheets were replaced every 30 s and the total testing time for each set of three samples was 600 s.

ASTM G76-89 was used to test the cermet coatings for resistance to small particle erosion. Compressed and filtered dry air at a pressure of 50 psi fed 50 μm angular alumina media through a 1.6 mm internal diameter nozzle. Erosion was normal to the coating surface. The media was blasted at a velocity of 60 m/s for 60 s onto as-sprayed surfaces of the coatings at a distance of 10 mm from the nozzle exit. The specimens were cleaned and weighed following erosion.

3. Results and Discussion

3.1 As-Received Powders

XRD analysis of the N-12 powder is shown in Fig. 1. All other powders exhibited equivalent phase composition, that of predominantly WC and also a small proportion of Co metal. SEM examination of the nanostructured powders revealed a hollow-sphere morphology with a number of the shells fragmented (Fig. 2a), though a small proportion of the particles also exhibited a solid sphere morphology. Higher magnification imaging of the shell surfaces highlighted discrete angular WC grains less than 1 μm in size (Fig. 2b).

3.2 Diagnostic Parameter Optimization

It should be noted that the temperature effects on coating properties are specific to this type of HVOF process and may differ significantly for other HVOF combustion processes. Although similar gas compositions may be used to produce equivalent flame temperatures, different systems allow for critical

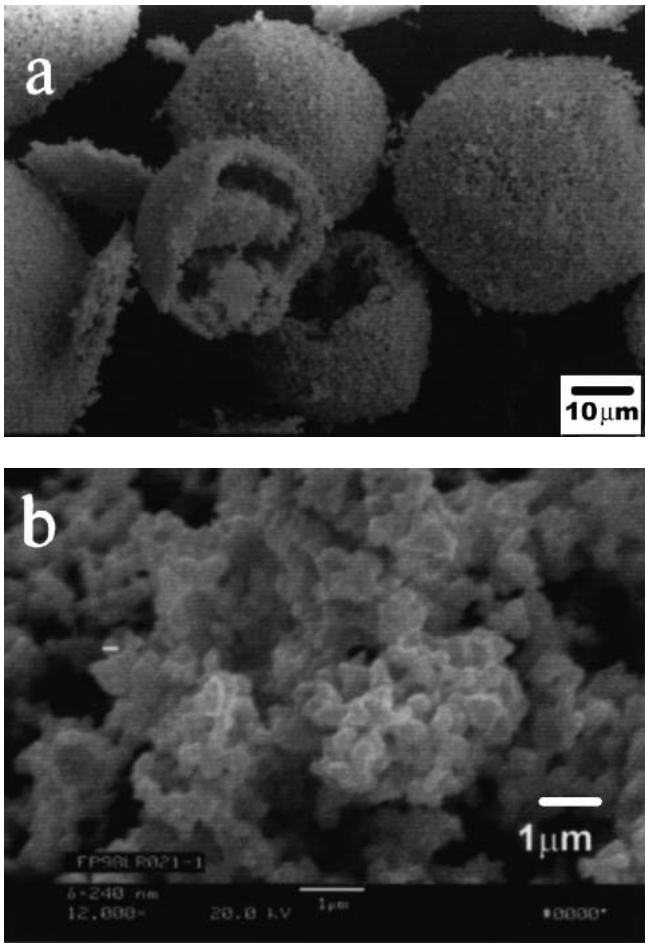

Fig. 2 SEM images of the as-received N-15 powder. **(a)** The hollow sphere morphology. **(b)** A high-magnification image of a particle surface showing discrete WC grains less than 1 μm in size

variations in factors such as position of powder injection and length of combustion region within the torch. Thus, the following explanation is pertinent to the DJ hybrid coating system and care must be taken before applying it to other HVOF coating systems.

The fuel-rich and oxygen-rich parameters presented in Table 3 were used to give similar particle velocities while reducing average particle temperatures. Data on flame temperatures for given propylene-to-oxygen ratios suggest that changes in gas chemistries as presented would not reduce particle temperatures to any great degree.[10] The average particle temperature reduction was thus achieved in part by an increase in the gas flow of the supplementary air, causing a greater throughput of gas while increasing the proportion of inert species (nitrogen) within the combustion plume. The particle temperatures and velocities at 125 mm (~5 in.) and 230 mm (~9 in.) distance from the nozzle exit are presented in Table 4 and show that the fuel-rich parameters gave average particle temperatures approximately 200 K lower than the standard condition at a standoff distance of 125 mm. The oxygen-rich parameters gave particle temperatures 50-100 K lower than the standard condition at 125 mm. The variation in particle temperatures between the three conditions was

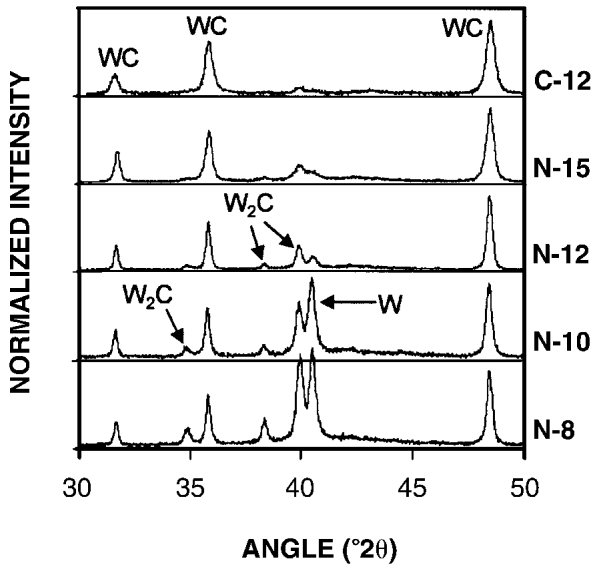

Fig. 3 XRD analyses of HVOF deposits of the materials studied

Table 4 Particle Temperatures and Velocities for the N-15 Material as a Function of Stoichiometric Ratio

Parameter	Stoichiometric Ratio, Fuel/Oxygen	Particle Temperature K		Particle Velocity, m/s	
		125 mm	230 mm	125 mm	230 mm
N-15FR	0.64	2207 ± 147	2163 ± 190	630 ± 123	534 ± 145
N-15	0.73	2390 ± 176	2278 ± 185	638 ± 103	553 ± 128
N-15OR	0.83	2329 ± 122	2239 ± 177	621 ± 99	522 ± 107

less at the substrate standoff distance (~230 mm). By monitoring the particle temperatures from the nozzle exit to the substrate, the maximum temperatures experienced generally are between 100 and 150 mm from the nozzle. Thus, the values presented at 125 mm are among the highest temperatures experienced by the particles in flight.

3.3 As-Deposited Coatings

The phase composition of the as-sprayed coatings differed significantly from that of the powders. Fig. 3 shows the coating XRD analyses for the four nanostructured cermets and in all cases, the presence of W_2C and W phases is clearly seen. Careful examination of the traces also reveals small diffuse humps at approximately 40° 2θ, which is known to be evidence of amorphization of the metallic Co phase.[11,12] The proportion of WC transformed to W_2C and W is significantly higher for all of the nanostructured cermets compared with the conventional coating.

The XRD analyses presented in Fig. 4 show the effect of varying the deposition parameters on the degradation of the WC phase. There is clearly a decrease in the decomposition of the WC phase and a corresponding decrease in the intensity of the W_2C and W peaks as the ratio of fuel to oxygen is increased. However, the highest degree of decomposition is seen for the N-15 condition. This is because this coating experiences the

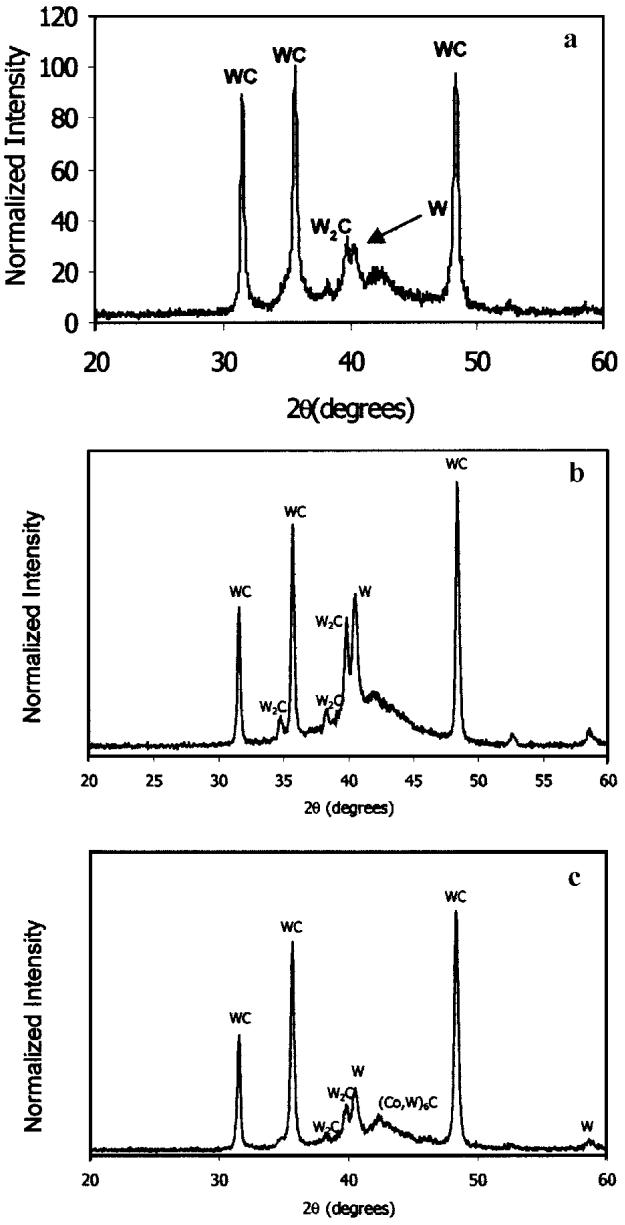

Fig. 4 XRD analyses of N-15 deposited using different spray parameters: **(a-c)** are from coatings deposited at the N-15OR, N-15, and N-15FR conditions, respectively.

highest overall particle temperatures during flight (see Table 4). Thus, it is clear that for these parameters, the temperature of the particles during deposition plays a more significant role than the oxygen-to-fuel ratio. The proportion of nanocrystalline/amorphous material in the deposit is also reduced on changing from a standard condition to either a more fuel-rich or oxygen-rich condition. From the diagnostic data, this corresponds to a reduction in maximum particle temperature on moving away from the standard condition. This would suggest that the proportion of amorphization of the metallic Co phase is more highly dependent upon the temperature the particles experience than the proportion of dissolution of W and C into the metal during spraying.

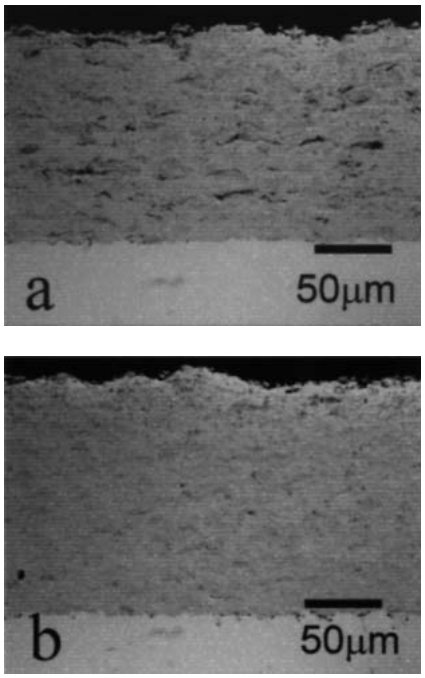

Fig. 5 **(a,b)** LM images of cross sections of the HVOF deposited N-8 and N-15 materials, respectively. Note the higher proportion of elongated pores within the N-8 coating.

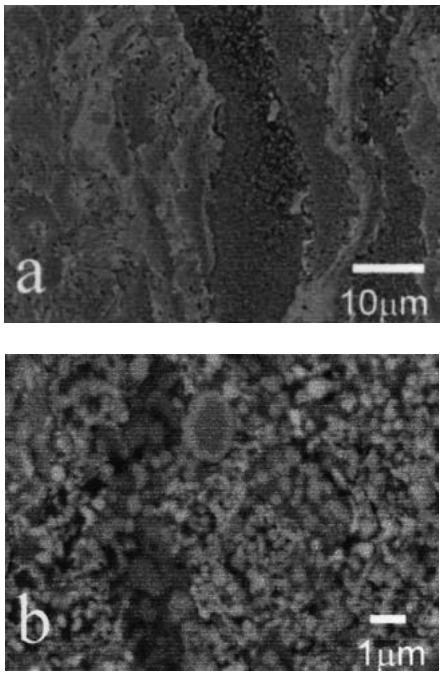

Fig. 6 **(a,b)** Low- and high-magnification SEM images, respectively, of a polished cross section of the N-12 sample

Table 5 Mechanical Property Data for the Coatings Studied

Specimen	Microhardness, HV_{300}	Surface Roughness, R_A	Abrasion Resistance, $mm^2 \cdot min/mm^3 \times 10^{-5}$	SPE Resistance, $mm^2 \cdot min/mm^3 \times 10^6$
N-8	1130 ± 116	2.9 ± 0.3	9.66 ± 0.39	4.050 ± 0.21
N-10	1105 ± 98	2.6 ± 0.4	9.27 ± 0.29	4.060 ± 0.09
N-12	1098 ± 122	2.6 ± 0.3	8.64 ± 0.54	4.118 ± 0.35
N-15	1100 ± 78	2.3 ± 0.2	7.87 ± 0.34	4.719 ± 0.22
N-15OR	1056 ± 134	2.9 ± 0.4	6.73 ± 0.31	…
N-15FR	1088 ± 112	2.7 ± 0.3	6.60 ± 0.45	…
C-12	1068 ± 37	4.0 ± 0.6	22.21 ± 0.50	6.635 ± 0.31

SPE, small particle erosion.

Figure 5 shows LM images of cross sections of the N-8 and N-15 sprayed coatings, respectively. Distinct layered splat morphology is seen for both coatings with variations in contrast within splats. There is a distinct difference in the degree of porosity within the two coatings; the N-8 exhibits significant elongated pores parallel to the substrate. The N-15 coating shows a much greater degree of consolidation with fewer pores visible. These elongated pores are believed to result from insufficient melting and flattening of the hollow porous spheres on impingement. The larger average particle sizes noted for the nanostructured powders may be responsible for this phenomenon.

The splat morphology observed in the LM study is seen in more detail in the BSE images of a cross section of the N-12 sprayed coating (Fig. 6a,b). There is distinct layering of the structure as well as variations in contrast within individual layers. It has been reported[13] that the layers of different contrast within the matrix regions are areas of varying W content, the W having dissolved from the WC particles during spraying. The higher magnification BSE image clearly shows distinct heavier atomic number particles within a matrix, although these particles are too fine for their exact morphology to be discerned.

The microhardness values for the coatings studied are presented in Table 5. There is no clear relationship between the microhardness of the nanostructured deposits and Co content. All of the coatings deposited under standard conditions exhibited hardnesses between approximately 1100 and 1200 values of hardness (VHN). These values are similar to the hardness values of the conventional WC coating. Lower hardnesses were found for the fuel-rich and oxygen-rich deposited coatings.

The surface roughness values presented in Table 5 show a greater smoothness for the nanostructured deposits compared with the conventional WC-sized cermet. This is likely to be due in part to the much finer average WC size of the nanostructured materials. There is also a reduction in roughness on increasing Co content consistent with a greater proportion of the molten metallic Co-rich phase.

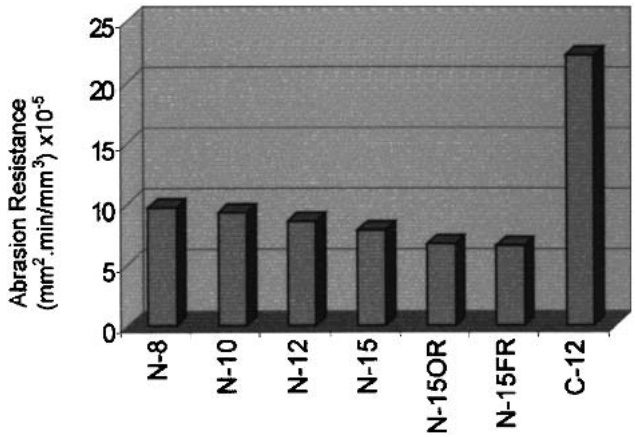

Fig. 7 Abrasion resistance for the sprayed deposits studied

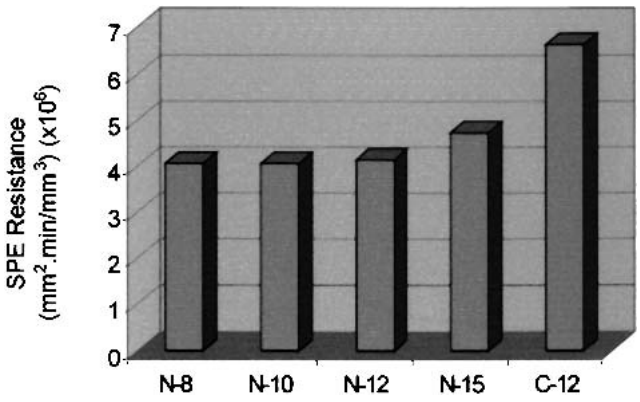

Fig. 8 Small-particle erosion data for the sprayed coatings studied

3.4 Abrasion Resistance

Table 5 and Fig. 7 present abrasion resistance data for the four nanostructured cermet coatings as well as a conventional WC sized coating. Included here also are data for the abrasion resistance for the parameter optimization study. The values were averaged from three specimens for each material. A clear trend can be seen with increased abrasion resistance on decreasing Co content. The most resistant nanostructured coating (N-8), however, exhibits approximately half the resistance of the conventional material. An equivalent trend of increased abrasion resistance on decreasing Co content was found by the authors to occur for conventional WC sized cermets deposited by HVOF.[14] This phenomenon is believed to be the result of an increased proportion of hard WC particles within the coating. However, from the phase analysis of the XRD data, it is clear that there also is an increased proportion of hard, brittle W_2C within the sprayed coating.

The abrasion resistance data for the oxygen- and fuel-rich conditions N-15OR and N-15OR are also presented in Table 5 and graphically in Fig. 7. A reduced resistance is seen for both conditions compared with the coating produced using standard conditions.

3.5 Small Particle Erosion

The effect of small particle erosion on the four nanostructured cermet coatings as well as a conventional WC sized coating is presented in Table 5 as well as the graph in Fig. 8. There is a general trend of decreasing erosion resistance on decreasing Co. The erosion resistance of the conventional coating was found to be superior to all of the nanostructured coatings. It has been shown for conventional sized WC cermets[15] that the small particle erosion resistance of HVOF deposited WC-Co cermets increases with reduced binder phase content (corresponding to a decreased binder mean free path). Higher Co contents increase the possibility of the eroding media contacting isolated binder phase areas causing a higher rate of material removal. However, for the nanostructured materials, there has been a clear increase in porosity as shown by the LM images in Fig. 5 as well as greater degradation of the WC phase within the lower Co content deposits. These factors are likely to play a significant role in reducing the small-particle erosion resistance of these materials.

The increased dissolution of the WC phase, both with a smaller average WC size, and also as the Co content is decreased, is shown clearly by this study. This result is consistent with other work[11] that relates the rate of the mechanism by which carbon is removed from the WC to the dissolution of the carbide grains, the diffusion of carbon toward the surface of the particles, and carbon oxidation at the surface. Clearly, a starting powder with finer carbides should lead to greater dissolution. In addition, a greater number of WC particles per unit area will increase this degree of degradation.

The greater amount of nanocrystalline/amorphous phase observed for the N-15 coating deposited under standard conditions compared with both the fuel- and oxygen-rich conditions is likely to be due to the higher particle temperatures achieved under the standard conditions. This would cause a greater amount of dissolution of W and C into the binder as well as a faster cooling rate of the binder phase. Both of these phenomena should result in a higher proportion of nanocrystalline/amorphous material.

It is clear that the improved abrasion resistance observed for nanostructured compared with conventional cemented carbides[4] is not found when these materials are deposited by HVOF. Stewart et al.[8] carried out three-body abrasive wear tests using both hard, angular abrading media and softer, more rounded media over a range of media sizes and counter body weights. They showed that the nanostructured coatings were more easily abraded by a mechanism of subsurface fracture within tungsten-rich regions of the binder phase. These regions are more prevalent in the nanostructured coatings, a result of higher surface area of WC leading to greater dissolution of this phase. This form of brittle fracture has also been observed in HVOF deposited WC-12Co, but has been claimed to be predominantly interlamellar.[16]

The increased abrasion resistance of the nanostructured cermets on decreasing Co content is believed to be due in part to shorter binder mean free paths (i.e., greater number of hard WC particles per unit area of exposed surface). This effect is seen to have a greater bearing on the abrasion resistance than the increased amount of dissolution of the WC phase for the lower Co content coatings. In addition, although there is greater porosity

within the lower cobalt coatings, the abrasion resistance is still greater. Note that the abrasion resistance of these materials has little relationship to the microhardness of the coatings as compared with the direct relationship between the two properties in cemented carbides.[4] It has been argued by Usmani et al.[14] that the abrasion resistance of HVOF deposited WC-Co coatings is directly related to their fracture toughness and inversely related to microhardness.

The reported decrease in small particle erosion resistance of conventional WC-Co on decreasing Co content[15] is not observed for the nanostructured coatings. It has been argued by Wayne and Sampath that a shorter binder mean free path in both cemented and thermally sprayed WC-Co materials increases the small particle erosion resistance. Smaller WC particles should result in a shorter binder mean free path for a given Co content exposing less isolated binder to the impinging media. However, from the XRD data, these particles are known to be more degraded, effectively increasing the mean free path of the binder as well as developing lower interfacial bond strengths between the binder and hard phase. The very much smaller size of the hard phase particles (20-200 nm) may also play a part in the reduced effectiveness of these coatings to withstand impinging alumina particles that are 50 μm in size.

Macroporosity and microsporosity play a significant role in reducing the erosion resistance of these materials.[17,18] The LM images shown in Fig. 4 suggest that there is greater porosity within these coatings compared with the conventional material; this maybe due in part to the hollow-sphere morphology and more porous nature of the nanostructured powders.

From the above findings, HVOF deposited nanostructured WC-Co cermets do not exhibit improved abrasion and small particle erosion resistance compared with conventional coatings. This is likely to be due to a number of factors that include but are not restricted to:

1) Starting powder morphology. The hollow sphere morphology produces coatings exhibiting higher porosity; specifically, elongated pores suggestive of insufficient flattening and melting of the particles. The larger size distribution of the powders must also increases the proportion of unmelted particles.
2) WC size distribution. The advantages of finer WC size distribution observed within cemented carbides do not translate to thermally sprayed coatings. The inherent increase in dissolution of the WC phase is believed to play a significant part in the reduction in wear resistance of these materials compared with conventional cermets.

Decreases in Co content from 15-8 wt.% give increases in abrasion resistance within these nanostructured coatings. However, the lower cobalt-containing deposits show higher porosity and are still significantly less resistant compared with conventional materials. Variations in the deposition parameter to reduce average particle temperatures while retaining velocity do not produce coatings with improved wear properties. This may be due in part to reduced particle melting, which reduces splat-splat interfacial strength.

4. Conclusions

1) It has been shown that increasing the cobalt content within HVOF deposited nanostructured cermet coatings reduces the ability of the deposit to withstand abrasion wear. This is consistent with a general trend observed for HVOF deposited conventional WC-sized cermet coatings.
2) Small-particle erosive wear resistance is increased on increasing Co content. This phenomenon is not consistent with findings for conventional WC-sized WC-Co coatings, suggesting that WC dissolution and macroporosity may play a significant role in the effectiveness of these deposits to resist small-particle damage.
3) Although decarburization of the deposit may be reduced on spraying by the use of more fuel-rich parameters, this does not improve the abrasion and small-particle erosion resistance of these nanostructured materials. This is believed to be due to a reduction in overall coating consolidation and splat-splat interfacial strength. This corresponds to a reduction in average particle temperatures for the fuel- and oxygen-rich deposition conditions of approximately 200 K compared with the standard condition.

Acknowledgments

This work was supported by the Office of Naval Research Grant number N000149910405 under the direction of Dr. Larry Kabacoff. The authors would also like to thank Dr. R. Sadangi for XRD analysis of some of the coatings.

References

1. B.H. Kear and L.E. McCandlish: "Chemical Processing and Properties of Nanostructured WC-Co Materials," *Nanostruct. Mater.*, 1993, *3*, pp. 19-30.
2. L.E. McCandlish, B.H. Kear, and B.K. Kim: "Chemical Processing of Nanophase WC-Co Composite Powders," *Mater. Sci. Technol.*, 1990, *6*, pp. 953.
3. K. Jia and T.E. Fischer: "Sliding Wear of Conventional and Nanostructured Cemented Carbides," *Wear*, 1997, *203-204*, pp. 310-18.
4. K. Jia and T.E. Fischer: "Abrasion Resistance of Conventional and Nanostructured Cemented Carbides," *Wear*, 1996, *200*, pp. 206-14.
5. M.R. Dorfman, B.A. Kushner, J. Nerz, and A.J. Rotolico: "A Technical Assessment of High-Velocity Oxygen-Fuel Versus High-Energy Plasma Tungsten Carbide-Cobalt Coatings for Wear Resistance" in *Proceedings 12th International Thermal Spray Conference*, I.A. Bucklow, ed., The Welding Institute, London, 1989, pp. 108.1-108.12
6. D.A. Stewart, A.H. Dent, S.J. Harris, A.J. Horlock, D.G. McCartney, and P.H. Shipway: "Novel Engineering Coatings with Nanocrystalline and Nanocomposite Structures by HVOF spraying," *J. Therm. Spray Technol.*, 1998, *7*(3), pp. 422-23.
7. S. Usmani, S. Sampath, and H. Herman: "HVOF Processing of Nanostructured WC-Co Coatings and Their Properties," *J. Therm. Spray Technol.*, 1998, *7*(3), pp. 429-30.
8. D.A. Stewart, P.H. Shipway, and D.G. McCartney: "Abrasive Wear Behavior of Conventional and Nanocomposite HVOF-sprayed WC-Co Coatings," *Wear*, 1999, *225-229*, p. 789.
9. Anon.: *Diamond Jet Process Manual*, Metco, Westbury, NY, 1991
10. A.D. Hewitt: "Technology of Oxy-Fuel Gas Processes. Part 2: Comparative Combustion Properties of Fuel Gases," *Weld. Met. Fabr.*, 1972, *11*, p. 382.
11. C. Verdon, A. Karimi, and J.-L. Martin: "A Study of High Velocity Oxy-fuel Thermally Sprayed Tungsten Carbide Based Coatings. Part 1: Microstructures," *Mater. Sci. Eng.*, 1998, *A246*, p. 11.
12. C.J. Li, A. Ohmori, and Y. Harada: "Formation of an Amorphous Phase

in Thermally Sprayed WC Co," *J. Therm. Spray Technol.*, 1996, *5*(1), pp. 69-73.

13. D.A. Stewart, P.H. Shipway, and D.G. McCartney: "Microstructural Evolution in Thermally Sprayed WC-Co Coatings: Comparison Between Nanocomposite and Conventional Starting Powders," *Acta Mater.*, 2000, *48*, p. 1593.
14. S. Usmani, S. Sampath, D.L. Houck, and D. Lee: "Effect of Carbide Grain Size on the Sliding and Abrasive Wear Behavior of Thermally Sprayed WC-Co Coatings," *Trib. Trans.*, 1997, *40*, p. 470.
15. S.F. Wayne and S. Sampath: "Structure/Property Relationships in Sintered and Thermally Sprayed WC-Co," *J. Therm. Spray Technol.*, 1992, *1*, p. 307.
16. A.C. Bozzi and J.D.B. deMello: "Wear Resistance and Wear Mechanisms of WC-12Co Thermal Sprayed Coatings in Three-Body Abrasion," *Wear*, 1999, *233-235*, pp. 575-87.
17. S. Rangaswamy: "Metallurgical Characterization of Plasma Sprayed Tungsten Carbide Cobalt Carbide Coatings," Ph.D. Thesis, State University of New York, Stony Brook, NY, 1987.
18. R.L. Mehan and J.R. Rairden: "Topical Report," Dept. Energy, DOE/MC/23174-2913, June 1990.